Journal of Hazardous Materials 162 (2009) 945–953

Contents lists available at ScienceDirect

Journal of Hazardous Materials

journal homepage: www.elsevier.com/locate/jhazmat

Titanium dioxide-mediated heterogeneous photocatalytic degradation of terbufos: Parameter study and reaction pathways

Ren-Jang Wu [b], Chiing-Chang Chen [a], Ming-Hung Chen [b], Chung-Shin Lu [a,*]

[a] Department of General Education, National Taichung Nursing College, Taichung 403, Taiwan, ROC
[b] Department of Applied Chemistry, Providence University, Taichung 433, Taiwan, ROC

ARTICLE INFO

Article history:
Received 26 February 2008
Received in revised form 24 May 2008
Accepted 26 May 2008
Available online 29 May 2008

Keywords:
Titanium dioxide
Organophosphorus pesticide
Terbufos

ABSTRACT

The photocatalytic degradation of terbufos in aqueous suspensions was investigated by using titanium dioxide (TiO_2) as a photocatalyst. About 99% of terbufos was degraded after UV irradiation for 90 min. Factors such as pH of the system, TiO_2 dosage, and presence of anions were found to influence the degradation rate. Photodegradation of terbufos by TiO_2/UV exhibited pseudo-first-order reaction kinetics, and a reaction quantum yield of 0.289. The electrical energy consumption per order of magnitude for photocatalytic degradation of terbufos was calculated and showed that a moderated efficiency (E_{EO} = 71 kWh/(m^3 order)) was obtained in TiO_2/UV process. To obtain a better understanding of the mechanistic details of this TiO_2-assisted photodegradation of terbufos with UV irradiation, the intermediates of the processes were separated, identified, and characterized by the solid-phase microextraction (SPME) and gas chromatography/mass spectrometry (GC/MS) technique. The probable photodegradation pathways were proposed and discussed.

1. Introduction

Organophosphorus pesticides (OPs) are widely used in modern agriculture as an alternative to organochlorines for pest control. This common class of compounds represents more than one-third of the total insecticides used in the world [1]. Due to their extensive use, OPs are currently present in surface natural waters. However, they are considered as extremely toxic compounds acting on acetylcholinesterase activity. This activity is also responsible for the toxicity in humans [2]. Several OPs and their degradation products have already been proven deleterious to aquatic fauna [3,4]. Therefore, the development of innovative technologies for the rapid degradation of OPs into environmentally compatible compounds is required.

Terbufos (*S*-*t*-butylthiomethyl-*O*,*O*-diethyl phosphorodithioate), an organophosphate pesticide, has been extensively used as a soil insecticide, especially in agriculture. Its chemical structure is shown in Fig. 1. It targets root pests that feed on corn, sugar beets, bananas, and other crops. Household uses include the control of cockroaches, houseflies, and termites along with the protection of plants of horticultural interest [5,6]. Terbufos is very toxic to aquatic organisms, with an acute LC50 for fish species ranging from 0.77 to 20 ppb [7,8]. Although terbufos was one of the extremely hazardous substances on the United States' Superfund National Priority List and was a candidate for the Draft Drinking Water Contaminant List that followed the Safe Drinking Water Act (1997), the United States alone consumed 4.5 millions pounds of terbufos in corn products in 1996 [9]. Terbufos is often detected in agricultural surface runoff waters [10], yet few studies on its treatment have appeared. In particular, studies focusing on its degradation products and pathways are lacking.

There are several methods of removing OPs from water, but each has shortcomings [11,12]. The adsorption method involves only a phase transfer of pollutants without degradation; the chemical oxidation method is unable to mineralize all organic substances; and in biological treatment methods the slow reaction rates and the disposal of activated sludge are the drawbacks to be considered [13,14]. Since organic pollutants can be completely degraded into harmless matter by photocatalysis under ambient temperature and pressure, scientists predict that it will soon be recognized as one of the most effective means of dealing with various kinds of wastewater [15].

The TiO_2-mediated photocatalysis process has been successfully used to degrade pollutants during the past few years [16–22]. TiO_2 is broadly used as a photocatalyst because of its non-toxicity, photochemical stability, and low cost [23]. The initial step in TiO_2-mediated photocatalysis degradation is proposed to involve the generation of an (e^-/h^+) pair, leading to the formation of hydroxyl radicals (•OH), superoxide radical anions ($O_2^{\bullet -}$), and hydroperoxyl

* Corresponding author. Tel.: +886 4 2219 6999; fax: +886 4 2219 4990.
E-mail address: cslu6@ntcnc.edu.tw (C.-S. Lu).

0304-3894/$ – see front matter © 2008 Elsevier B.V. All rights reserved.
doi:10.1016/j.jhazmat.2008.05.121

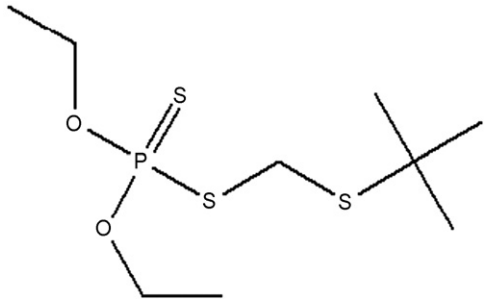

Fig. 1. Chemical structure of terbufos.

radicals (•OOH) as shown below [24–26]:

$$TiO_2 + h\nu \rightarrow TiO_2(h^+ + e^-) \quad (1)$$

$$H_2O_{(ads)} + h^+ \rightarrow {}^\bullet OH + H^+ \quad (2)$$

$$OH^- + h^+ \rightarrow {}^\bullet OH \quad (3)$$

$$O_2 + e^- \rightarrow O_2{}^{\bullet -} \quad (4)$$

$$O_{2(ads)} + e^- + H^+ \rightarrow HO_2{}^\bullet \quad (5)$$

The organic pollutants are attacked and oxidized by the radicals formed through the above mechanisms. In addition to hydroxyl radicals, superoxide radical anions – and in some cases the positive holes – are also suggested as possible oxidizing species that could attack organic compounds present at or near the surface of TiO_2 [27].

O'Shea et al. [28] indicated that the TiO_2 photocatalytic degradation of dimethyl methyl phosphonate (DMMP) could be accomplished in an oxygenated aqueous solution. Final degradation products of the DMMP are phosphoric acid and CO_2. Malato et al. [29] demonstrated that TiO_2 photocatalyzed mineralization of methamidophos occurs in aqueous solutions under solar irradiation. Kerzhentsev et al. [30] analyzed the photocatalytic oxidation of fenitrothion using TiO_2 suspensions. They detected several intermediate organic compounds that were completely mineralized to CO_2, $H_2PO_4{}^-$, $SO_4{}^{2-}$ and $NO_3{}^-$. Konstantinou et al. [31] studied the photocatalytic oxidation of several other OPs (ethyl parathion, methyl parathion, dichlorofenthion, and ethyl bromophos) in aqueous TiO_2 suspensions. Some of the major intermediate products of photodegradation were identified by means of mass spectrometry. Sakkas et al. [32] reported the application of solid-phase microextraction for monitoring the photocatalytic degradation of ethyl parathion in aqueous TiO_2 suspensions. Some of the intermediate products were successfully extracted with the SPME technique and identified by combined gas chromatography/mass spectrometry (GC/MS). Moctezuma et al. [11] investigated the photocatalytic degradation of methyl parathion in aqueous TiO_2 suspensions and identified the intermediate products using a number of analytical techniques.

At present, no studies on the removal of terbufos have been reported, and a detailed study of the photocatalytic degradation process might provide useful information for the use of TiO_2 in the treatment of terbufos in aqueous solution. In our study, various parameters that may affect the photodegradation of terbufos in the presence of TiO_2 suspensions were analyzed, in order to obtain a more complete knowledge of TiO_2 photocatalytic efficiency. This study also focused on the identification of the reaction intermediates and understanding of the mechanistic details of the photodegradation of terbufos in the TiO_2/UV light process as a foundation for future application of this energy saving technology.

2. Experimental

2.1. Materials and reagents

Terbufos (98.6%) was obtained from Sigma–Aldrich. Standard solutions containing 5 mg L^{-1} of terbufos in water were prepared, protected from light, and stored at 4 °C. Di-*tert*-butyl disulfide (Sigma–Aldrich), *tert*-butanol (Merck), and acetone (J.T. Baker) were used for intermediate confirmation. Other chemicals were of reagent grade and used as such without further purification. The TiO_2 nanoparticles (P25, ca. 80% anatase, 20% rutile; particle size, ca. 20–30 nm; BET area, ca. 55 $m^2\,g^{-1}$) were supplied by Degussa. De-ionized water was used throughout this study. The water was purified with a Milli-Q water ion-exchange system (Millipore Co.) to give a resistivity of $1.8 \times 10^7\ \Omega$ cm.

Caution! Extreme care should be taken when using the terbufos since it is classified as toxicity class I—highly toxic [7]. Exposure of terbufos to the researcher is possible by inhalation of air contaminated by release during the preparation of the standard solution. All work must be done in a hood. Rubber gloves should be worn whenever this reagent is handled.

2.2. Apparatus and instruments

The apparatus for studying the photocatalytic degradation of terbufos has been described elsewhere [33]. The C-75 Chromato-Vue cabinet of UVP provides a wide area of illumination from the 15 W UV-365 nm tubes positioned on two sides of the cabinet interior. Solid-phase microextraction was utilized for the analysis of terbufos and intermediates resulting from the photocatalytic degradation process. SPME holder and fiber-coating divinylbenzene-carboxen-polydimethylsiloxane (DVB-CAR-PDMS 50/30 μm) were supplied from Supelco (Bellefonte, PA). GC/MS analyses were run on a PerkinElmer AutoSystem-XL gas chromatograph interfaced to a TurboMass selective mass detector. The ionic by-products from terbufos degradation were analyzed using a Dionex ICS-90 ion chromatograph.

2.3. Procedures and analysis

An aqueous TiO_2 dispersion was prepared by adding 50 mg of TiO_2 powder to a 100-mL solution containing terbufos at appropriate concentrations. For reactions in different pH media, the initial pH of the suspensions was adjusted by addition of either NaOH or HNO_3 solutions. Prior to irradiation, the dispersions were magnetically stirred in the dark for 30 min to ensure the establishment of the adsorption/desorption equilibrium. Irradiations were carried out using two UV-365 nm lamps (15 W). After each irradiation cycle, the amount of terbufos was thus determined by SPME-GC/MS. The aqueous TiO_2 dispersion was sampled (5 mL) and centrifuged to separate the TiO_2 particles. The clear solution was then transferred into 4 mL sample vial. The SPME fiber was directly immerged into the sample solution to extract terbufos and its intermediates for 30 min at room temperature, with magnetic stirring at 550 ± 10 rpm on the Corning stirrer/plate (Corning, USA). Finally, the compounds were thermally desorbed from the fiber to the GC injector for 40 min. Separation was carried out in a DB-5 capillary column (5% diphenyl/95% dimethyl-siloxane), 60 m, 0.25-mm i.d., and 1.0-μm thick film. A split–splitless injector was used under the following conditions: injector temperature 250 °C, split flow 10 mL/min. The helium carrier gas flow was 1.5 mL/min. The oven temperature program was 1.0 min at 60 °C, 8 °C/min to 240 °C (16.5 min). Electron impact (EI) mass spectra were monitored from 10 to 350 *m*/*z*. The ion source and inlet line temperatures were set at 220 and 250 °C, respectively.

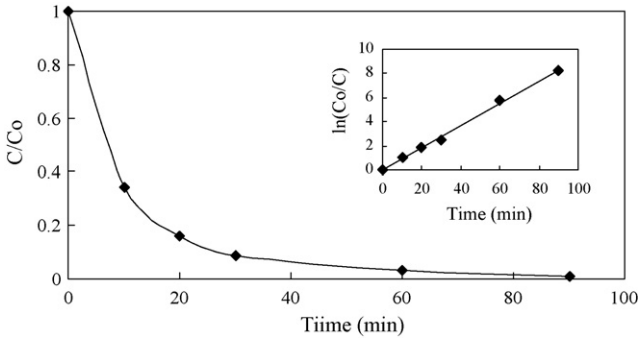

Fig. 2. Photodegradation kinetics of terbufos in the presence of TiO_2 particles. Experimental condition: terbufos concentration 5 mg L^{-1}; TiO_2 concentration 0.5 g L^{-1}; pH 6.

The ionic by-products from terbufos degradation were analyzed using a Dionex ICS-90 ion chromatograph. The column was an IonPac® AS4A-SC (4 mm × 250 mm) for phosphate (PO_4^{3-}) and sulfate (SO_4^{2-}) analyses. The flow rate was 1.0 mL/min, and the injection volume was 100 μL of the filtered reaction samples. The eluent consist of a mixture of 3.5 mM Na_2CO_3 and 1 mM $NaHCO_3$ for the anion analysis. For these operating conditions, the retention times for PO_4^{3-} and SO_4^{2-} were 5.4 and 6.7 min, respectively. For quantitative studies, standard solutions and calibration curves for each ion were prepared in the range from 1 to 10 mg L^{-1}. In order to avoid adsorbed processes of the anions on the surface of the catalyst during the reaction progress, a desorption procedure was applied. This consisted of the addition of NaOH (1N) to the reaction mixture after irradiation until it had reached a pH of 12.

3. Results and discussion

3.1. Photodegradation kinetics

The photocatalytic degradation of terbufos is presented in Fig. 2 while, in the inset, the logarithm of the ratio of the initial concentration (C_0) to the concentration at a given time (C) versus time (t) is plotted. The rate constant (k_{app}) was determined by calculating the slope of the line obtained. About 99% of the terbufos was degraded after UV irradiation for 90 min. Table 1 lists the calculated values of k_{app} and the linear regression coefficients for the pseudo-first-order kinetics of the photodegradation of the studied compound. Based on these values the appropriate first-order relationship appears to fit well [34,35].

3.2. pH effect

Several control experiments, at the same initial concentrations as the photocatalytic experiments, were performed to guarantee that the results obtained during the photocatalytic tests were consistent and not due to hydrolysis. The results indicated that only slight hydrolysis was detected after 3 h in solutions kept in the dark at pH 4 and 8 (see Fig. 3). Photocatalytic degradation of terbufos by TiO_2 obtained in this study is much faster than hydrolysis. The contribution of hydrolysis is negligible.

Table 1
Photodegradation kinetics parameters (rate constants and linear regression coefficients R^2) for terbufos in the presence of TiO_2 (0.5 g L^{-1})

pH	K_{app} (min^{-1})	R^2
3	0.0616	0.966
4	0.0768	0.993
6	0.0814	0.985
8	0.0854	0.995

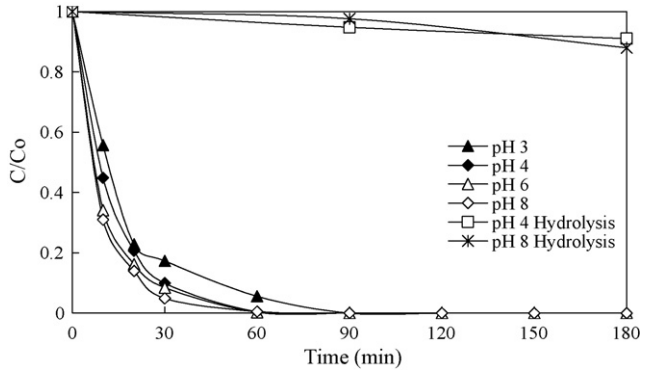

Fig. 3. pH effect on the photodegradation rate of terbufos with concentration of TiO_2 at 0.5 g L^{-1} and terbufos at 5 mg L^{-1}.

Many studies have indicated that the pH of a solution is an important parameter in the photocatalytic degradation of organic compounds. This is because pH influences the surface charge of the semiconductor, thereby affecting the interfacial electron transfer and the photoredox process [36]. The influence of the initial pH value on the photodegradation rate of terbufos for the TiO_2 suspensions is demonstrated in Fig. 3. The results indicated that the degradation rate decreased with a decrease in pH, and it proceeded much faster under an alkaline pH. The effect of pH on a photocatalytic reaction is generally ascribed to the surface charge of the photocatalyst and its relation to the ionic form of the organic compound (anionic or cationic). Electrostatic attraction or repulsion between the photocatalyst's surface and the organic molecule is taking place, and these events consequently enhance or inhibit, respectively, the photodegradation rate [37]. Since terbufos is a unionizable compound, the observed increase of the degradation rate under an alkaline pH can be attributed to the high hydroxylation of the photocatalyst's surface due to the presence of a large quantity of OH^- ions. Consequently, a higher concentration of $^{\bullet}OH$ species is formed, and the overall rate is enhanced.

3.3. Effect of TiO_2 dosage

It is important from both the mechanistic and application points of view to study the dependence of the photocatalytic reaction rate on the concentration of TiO_2. Hence, the effect of TiO_2 dosage on the photodegradation rate of terbufos was investigated by employing different concentrations of TiO_2 varying from 0.1 to 2.0 g L^{-1}. The photocatalytic degradation rate was found to increase with increasing TiO_2 dosages, but the reaction was retarded at high TiO_2 dosages (Fig. 4). The increase in the rate was likely due to the increase in the total surface area (or number of active sites) available for photocatalytic reaction as the dosage of TiO_2 increased. However, when TiO_2 was overdosed, the intensity of incident UV light was attenuated because of the decreased light penetration and increased light scattering, which counteracted the positive effect coming from the dosage increment and therefore reduced the overall performance [38–40].

3.4. Effects of anions

The study of the effects of anions on the photocatalytic degradation of terbufos is important because anions are often present in natural water systems. The effects of Cl^- and NO_3^- ions on the degradation rate of terbufos were examined individually by adding NaCl and $NaNO_3$ to the system until the resultant solution contained 0.05 M of Cl^- and NO_3^- ions before the irradiation had begun. The results showed that anions inhibited the degradation

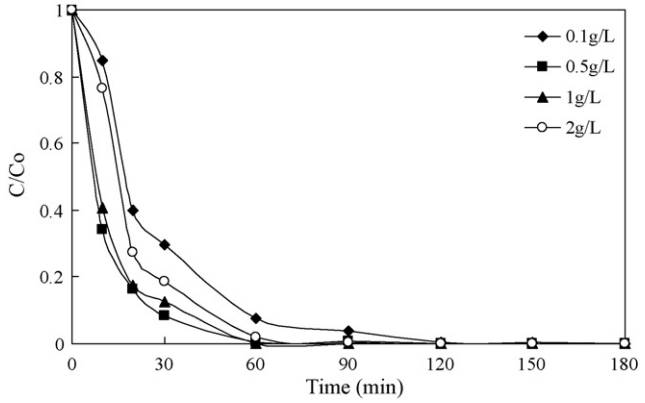

Fig. 4. Effect of TiO_2 dosage on the photodegradation rate of terbufos. Experimental condition: terbufos concentration 5 mg L^{-1}; pH 6.

considerably (see Fig. 5). The inhibition effects of anions can be explained as the reaction of positive holes and hydroxyl radical with anions that behaved as h^+ and •OH radical scavengers (Eqs. (6) and (7)), resulting in prolonged terbufos removal. Probably, the adsorbed anions compete with terbufos for the photo-oxidizing species on the surface and prevent the photocatalytic degradation of terbufos. Formation of inorganic radical anions (e.g., Cl•, $ClOH^{-}$•) under these circumstances is possible.

$$Cl^- + h^+ \rightarrow Cl^{\bullet} \quad (6)$$

$$Cl^- + {}^{\bullet}OH \rightarrow ClOH^{-\bullet} \quad (7)$$

Although the reactivity of these radicals may be considered, they are not as reactive as h^+ and •OH, and thus the observed retardation effect is still thought to be the strong adsorption of the anions on the TiO_2 surface [41]. Similar results have been reported previously by Chen et al. [42], suggesting that inorganic anions were capable of inhibiting the photocatalytic degradation of dichloroethane in aqueous suspensions of TiO_2.

3.5. Formation of ionic by-products

Since terbufos is a phosphorodithioate pesticide containing sulfur and phosphorus atoms, the sulfate (SO_4^{2-}) and phosphate (PO_4^{3-}) are potential ionic degradation by-products. An alternative approach to tracking the progress of the TiO_2 photocatalytic degradation of terbufos is to monitor the SO_4^{2-} and PO_4^{3-} formed in the solution. Therefore, we measured the ionic by-products produced during photocatalysis. Preliminary results showed that PO_4^{3-} was

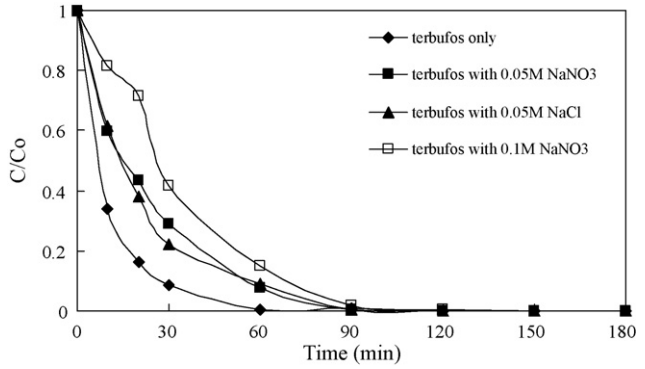

Fig. 5. Effect of anions on the photocatalytic degradation of terbufos in water. Experimental condition: terbufos concentration 5 mg L^{-1}; TiO_2 concentration 0.5 g L^{-1}; pH 6.

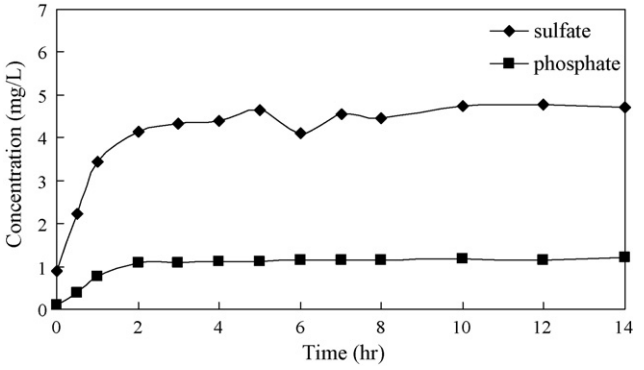

Fig. 6. Evolution of sulfate and phosphate anions originating from terbufos photocatalytic degradation. Experimental condition: terbufos concentration 5 mg L^{-1}; TiO_2 concentration 0.5 g L^{-1}; pH 6.

retained on the surface of TiO_2 in the degradative process. The adsorption of phosphate ions onto the surface of the photocatalyst has already been reported [43,44]. Therefore, a procedure to desorb these compounds was applied (see Section 2 for the correct evaluation of the formation of these ions).

The evolutions of ionic by-products as a function of irradiation time are shown in Fig. 6. Ion chromatography analysis shows the increase of sulfate and phosphate concentrations in the reaction mixture as the photocatalysis progressed. The increase indicates that sulfur and phosphorus atoms were oxidized to sulfate and phosphate ions, respectively, after they were released from the terbufos molecule. However, the formation profiles of sulfate and phosphate ions indicate that the reaction does not go to completion. In fact, only about 94% of the initial organic sulfur and 73% of the initial organic phosphorus have been transformed into SO_4^{2-} and PO_4^{3-}, respectively, implying that other less volatile organic compounds still inhabited the irradiated solution because only volatile products, sulfates and phosphates were identified and measured.

3.6. Separation and identification of the intermediates

Since most organophosphorus pesticides are usually sparingly soluble in water [45], it was therefore a challenge to study their photodegradation in dilute aqueous solutions in the absence of any organic solvents, and to identify their degradation products. A relatively low intensity UV-365 lamp (15 W) was used in our study for the identification of organic intermediates. This enabled us to obtain slower degradation rates and provide favorable conditions for the determination of intermediates. Additionally, the initial terbufos concentration (5 mg L^{-1}) was selected to be high enough to facilitate the identification of intermediate products.

Temporal variations occurring in the terbufos solution during the photocatalytic degradation process with UV irradiation were examined with SPME-GC/MS. Fig. 7 displays the chromatogram of the reacted solution during irradiation in the presence of TiO_2. With irradiation up to 30 min, nine components were identified, all with retention times less than 40 min. One of the peaks was the initial terbufos (peak I); the other eight (new) peaks were the intermediates formed. We denoted the terbufos and its related intermediates as species I–IX. Table 2 summarizes the identified intermediates of terbufos along with their retention times and the characteristic ions of the mass spectra. Except for the initial terbufos, the other peaks increased at first and subsequently decreased, indicating formation and subsequent transformation of the intermediates. Some other minor peaks were present, but mass fragment information did not allow elucidation of their structures.

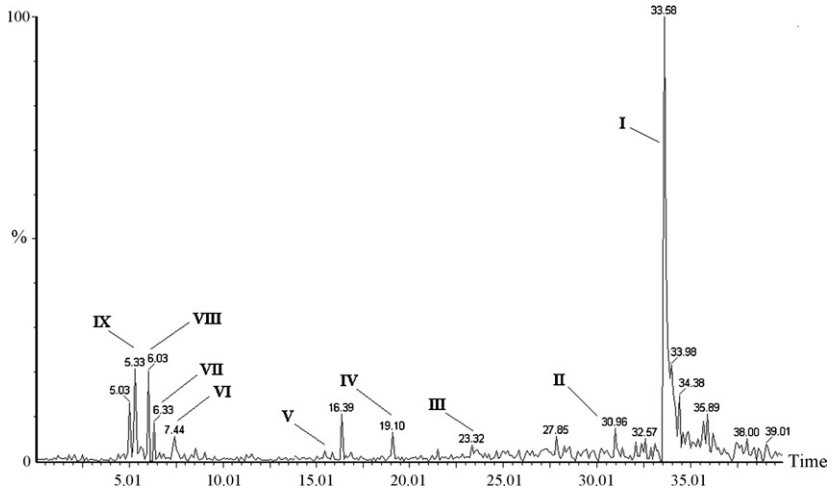

Fig. 7. GC/MS chromatogram obtained for terbufos solution after 30 min of irradiation with UV light in the presence of TiO_2.

Fig. 8 shows the mass spectra of intermediates formed during the photocatalytic degradation of terbufos in the presence of TiO_2 ($0.5\,g\,L^{-1}$) particles. Compound II, which was identified as terbufos-oxon, exhibits a peak at $m/z = 272$ which corresponds to the molecular ion $[M]^+$ and the characteristic ions at $m/z = 215$, $m/z = 171$, and $m/z = 57$ that correspond to the groups $[(C_2H_5O)_2POSCH_2S]^+$, $[(C_2H_5O)POHSCH_2S]^+$ and $[(CH_3)_3C]^+$, respectively. Terbufos-oxon has been identified, in a previous study, as a terbufos metabolite formed in vivo in studies with animals [46]. Compound II was further identified by comparing the mass spectrum with previous reported spectrum. The fragments of the studied compound match with the previous spectrum of the literature.

Compound III, which was identified as *O,O*-diethyl phosphorodithioic ester, exhibits a peak at $m/z = 186$ which corresponds to the molecular ion $[M]^+$ and the characteristic ions at $m/z = 153$, $m/z = 125$, and $m/z = 97$ that correspond to the groups $[(C_2H_5O)_2P(S)]^+$, $[(C_2H_5O)P(S)(OH)]^+$ and $[(HO)_2P(S)]^+$, respectively. This compound was also identified, in a previous study, as a by-product of terbufos hydrolysis [9].

A search of the mass spectra library selected di-*tert*-butyl disulfide as a good match (89%) for compound IV, whose retention time on GC was 19.10 min. Neat di-*tert*-butyl disulfide, purchased from Aldrich and dissolved in methanol, yielded the same GC retention time (~19.15 min) and mass spectrum as that of the suspected di-*tert*-butyl disulfide found in the irradiated samples of the terbufos photocatalytic experiment. Di-*tert*-butyl disulfide is an interesting intermediate because it most likely forms from the dimerization of *tert*-butanethiol (a molecular segment of terbufos's side chain).

The molecular mass of compound V was determined from the chemical ionization mass spectrum to be $m/z = 120$ by the observation of an $[M+H]^+$ ion of 121. The EI mass spectrum of this compound showed the characteristic ion at $m/z = 89$ that corresponded to the loss of an aliphatic alcohol $[CH_2{=}OH]^+$ fragment. The base peak at $m/z = 57$ in the mass spectrum corresponded to the *tert*-butyl moiety. Based on these data, the structure of compound V was identified as *tert*-butyl-hydroxymethyl sulfide. As the pure compound is not commercially available, a more conclusive identification is difficult.

Compound VI was identified as *tert*-butanethiol by a library search with a fit value of 91%. The mass spectrum of this compound showed a peak at $m/z = 90$ which corresponds to the molecular ion $[M]^+$ and the characteristic ions at $m/z = 75$ and $m/z = 57$ that correspond to the groups $[(CH_3)_2C{=}SH]^+$ and $[(CH_3)_3C]^+$, respectively. Compounds VII and VIII were identified as *tert*-butanol and acetone with fit values of 84 and 94%, respectively, found by searching the mass spectra library. Both compounds were further identified by matching their retention times and mass spectra with those of an authentic standard. They exhibit the exact retention times and similar mass spectra. A trace of isobutene (compound IX) was detected as a degradation product with a fit value of 87% during the photocatalytic reaction of terbufos.

3.7. Initial photooxidation pathway

It is well established that conduction band electrons (e^-) and valence band holes (h^+) are generated when an aqueous TiO_2 suspension is irradiated with light energy greater than its band gap energy (3.2 eV). The hydroxyl radicals can be produced by oxidation of water by holes. Nakamura and Nakato [47] proposed a mechanism of water oxidation by a nucleophilic attack to a surface-trapped hole at a bridged O site. Murakami et al. [48] reported

Table 2
Identification of the intermediates from the photodegradation of terbufos by GC/MS

Peaks	Photodegradation intermediates	R.T. (min)	MS peaks (m/z)
I	Terbufos	33.58	288,231,153,125,97,65,57,41
II	Terbufos-oxon	30.96	272,215,171,143,115,57
III	*O,O*-Diethyl-phosphorodithioic ester	23.32	186,153,125,97,65,45
IV	Di-*tert*-butyl disulfide	19.10	178,122,57,41
V	*tert*-Butyl-hydroxymethyl sulfide	15.48	120,89,57,41
VI	*tert*-Butanethiol	7.44	90,75,57,41
VII	*tert*-Butanol	6.33	74,59,41,31
VIII	Acetone	6.03	58,43,15
IX	Isobutene	5.33	56,41,27

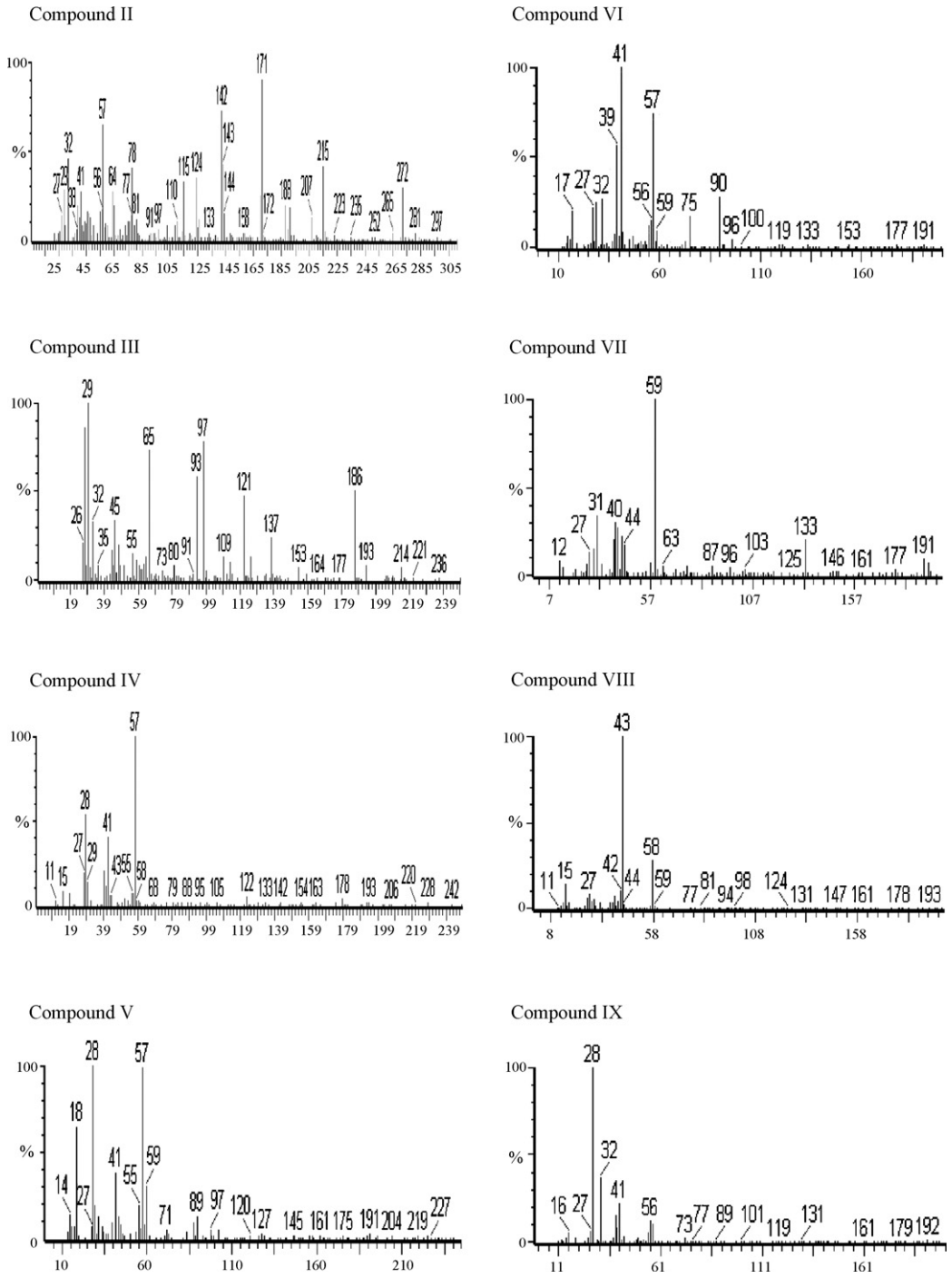

Fig. 8. Mass spectra of intermediates formed during the photodegradation of terbufos after they were separated by GC/MS method.

when the O–O bond in Ti–O–OH breaks the hydroxyl radicals can be formed from the bridge OH groups.

$$[\text{Ti–O–Ti}]_s + h^+ + H_2O \rightarrow [\text{Ti–O}^\bullet\text{HO–Ti}]_s + H^+ \quad (8)$$

$$[\text{Ti–O}^\bullet\text{HO–Ti}]_s \rightarrow [\text{Ti–O–O–Ti}]_s + H^+ \quad (9)$$

$$[\text{Ti–O–O–Ti}]_s + H_2O \rightarrow [\text{Ti–O–OH}^\bullet\text{HO–Ti}]_s \quad (10)$$

$$[\text{Ti–O–OH}^\bullet\text{HO–Ti}]_s \rightarrow [\text{Ti–O}^\bullet\text{HO–Ti}]_s + {}^\bullet\text{OH} \quad (11)$$

Two oxidative agents can be considered: the photo-produced holes (h^+) and the hydroxyl radicals ($^\bullet$OH) which are known as strongly active non-selective agents responsible for the heterogeneous TiO_2 photodecomposition of organic substrates. Scheme 1 shows the proposed mechanism for the generation of the primary detected intermediates. The formation of terbufos-oxon (compound II) is attributed to oxidative desulfuration by $^\bullet$OH attack (Scheme 1, route A). Terbufos-oxon represents one of the most expected intermediates since previous studies showed that the oxidant attack of the $^\bullet$OH radicals on the P=S bond occurs firstly in the case of phosphorothioates, resulting to the formation of the oxon derivatives [30,34,49,50].

In addition to the degradation route of P=S bond destruction, an alternative pathway was also identified. First, oxidation of the terbufos molecule to form the terbufos cation radical takes place

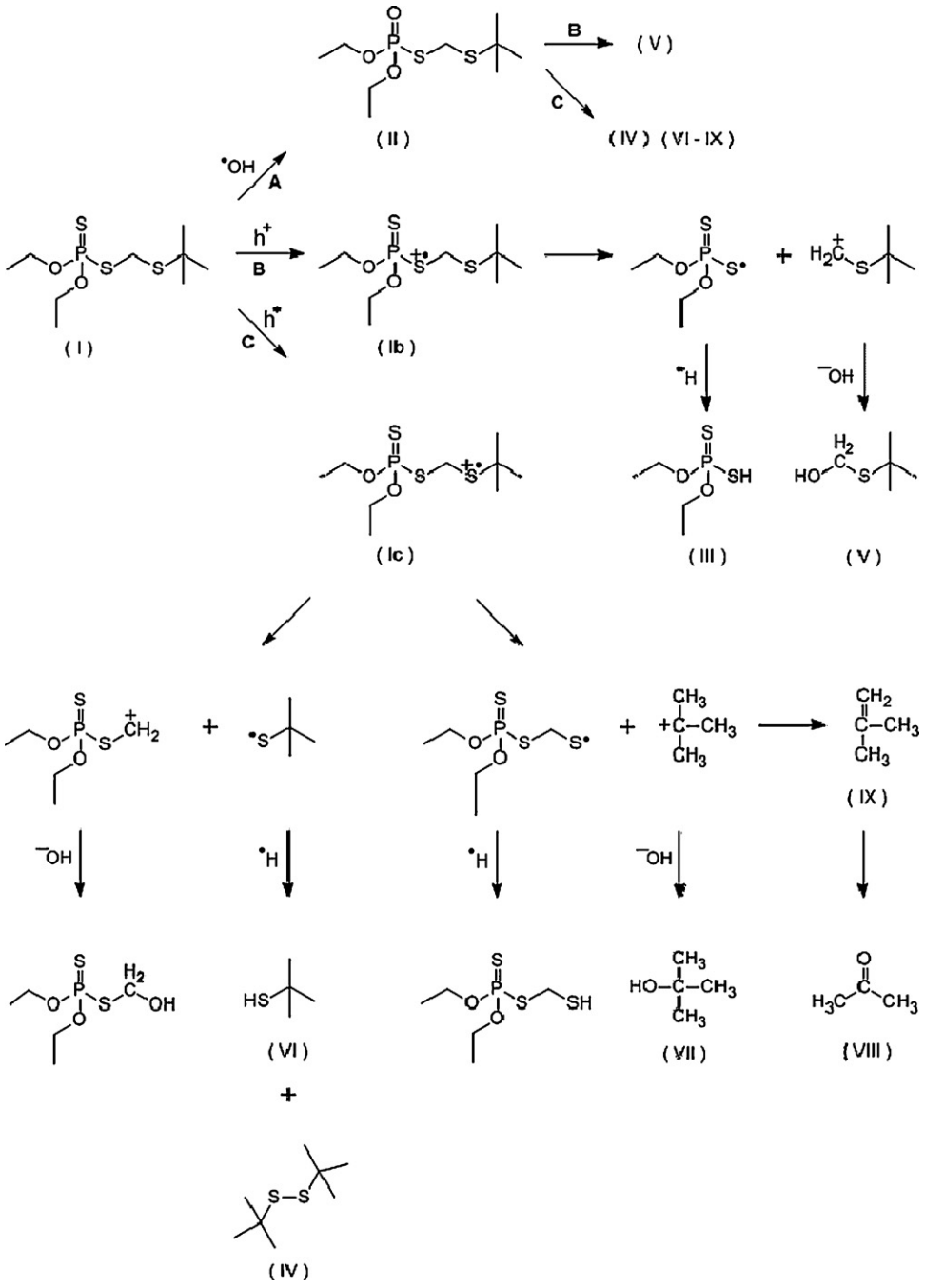

Scheme 1. Proposed photodegradation pathway of terbufos under UV irradiation in aqueous TiO_2 dispersions.

when positive holes attack it, initiating a series of reactions. The formation of cation radicals has also been observed in the photocatalytic degradation of other organophosphorus pesticides [34], thiocarbamate pesticides [51], and thioethers [52]. The interfacial transfer of a single electron from the sulfur atom, located near the phosphorus atom, leads to the formation of terbufos cation radical **1b** (Scheme 1, route B). The scission of the C—S bond in this cation radical leads to the formation of $(C_2H_5O)_2P(S)S^\bullet$ radicals that are the precursor of *O*,*O*-diethyl phosphorodithioic ester (compound III). The H atoms necessary to S—H bond formation were proposed to have originated from the proton reduction by photogenerated electrons $H^+ + e^- \rightarrow H^\bullet$ as already observed in the degradation of the insecticide fenitrothion by Kerzhentsev et al. [30]. Similarly, *tert*-butyl-hydroxymethyl sulfide (compound V) is formed by the scission of the C—S bond in the terbufos cation radical **1b** through a hydrolytic pathway.

The interfacial transfer of a single electron from the sulfur atom, which is located far from the phosphorus atom, leads to the formation of terbufos cation radical **1c** (Scheme 1, route C). The scission of the C—S bond in this cation radical leads to the formation of $^\bullet SC(CH_3)_3$ radicals that are the precursor of *tert*-butanethiol (compound VI). The recombination of $^\bullet SC(CH_3)_3$ radicals could form dimers such as di-*tert*-butyl disulfide (compound IV). The dimerization of thiol radicals has been reported also in the case of the photocatalytic degradation of thiocarbamate pesticides [53]. In addition, disulfides have been detected during the oxidation of

similar organophosphorus insecticide molecules such as disulfoton and phorate [54,55] through hydrolysis. The formation of disulfide could also be attributed to the oxidation of the resulting thiol by oxygen as reported elsewhere [55]. Similarly, the scission of the C—S bond in the terbufos cation radical **1c** leads to the formation of *tert*-butyl carbonium ion. The carbocation is extremely unstable and undergoes rapid hydrolysis and dehydrogenation. Hydrolysis of *tert*-butyl carbonium ion yields *tert*-butanol (compound VII) while the dehydrogenation leads to the formation of isobutene (compound IX). Subsequently, isobutene undergoes oxidation to acetone (compound VIII) [56].

3.8. Relative photonic efficiency and quantum yield

Quantum yield is an important parameter in photochemistry. Its precise measurement is often difficult in a heterogeneous dispersion owing to non-negligible scattering of the light irradiance impinging on the reactor [57]. Considering the difficulty of quantum yield measurements, phenol was selected as a standard secondary actinometer to assess the relative photonic efficiency (ξ_{rel}) of the photodegradation of terbufos against phenol according to the protocol reported by Serpone et al. [58]. In our study, the relative photonic efficiency ξ_{rel} was 2.63 determined under identical experimental conditions (initial concentration of reactant, 0.017 mM (100 mL); TiO_2 loading, 0.5 g L^{-1} (P25); pH 6). The quantum yield can subsequently be determined from ξ_{rel}, as $\Phi_{terbufos} = \xi_{rel}\Phi_{phenol}$, where Φ_{phenol} is the quantum yield for the photocatalyzed oxidative disappearance of phenol using Degussa P25 TiO_2 as the standard catalyst material. The quantum yield of photodegradation of phenol has been determined ($\Phi_{phenol} = 0.11 \pm 0.01$) by Serpone et al. [59]. Therefore, actinometer studies resulted in a reaction quantum yield for terbufos of 0.289.

3.9. Electrical energy efficiency

Recently the international union of pure and applied chemistry (IUPAC) has proposed two figures-of-merit for advanced oxidation processes (AOPs) on the use of electrical energy. In the case of low pollutant concentrations (which applies here), the appropriate figure-of-merit is the *electrical energy per order* (E_{EO}), defined as the number of kilowatt hours of electrical energy required to reduce the concentration of a pollutant by 1 order of magnitude (90%) in 1 m^3 of contaminated water. The E_{EO} (kWh/(m^3 order)) can be calculated from the following equations [60]:

$$E_{EO} = \frac{P \times t \times 1000}{V \times 60 \times \log(C_0/C)} \quad (12)$$

$$E_{EO} = \frac{38.4 \times P}{V k_{app}} \quad (13)$$

where P is the power input (kW) from the wall to drive the UV lamp, t is the irradiation time (min), V is the volume (L) of the water in the reactor, Co and C are the initial and final pollutant concentrations, and k_{app} is the pseudo-first-order rate constant (min^{-1}) for the decay of the pollutant concentration. The degradation of terbufos was found to follow pseudo-first-order kinetics, and hence the figure-of-merit electrical energy per order (E_{EO}) is appropriate for estimating the electrical energy efficiency. Our study shows that terbufos can be treated easily and effectively with the TiO_2/UV process with E_{EO} value of 71 kWh/(m^3 order).

4. Conclusion

Terbufos could be successfully degraded by TiO_2 under UV irradiation. After a 15-W UV-365 nm irradiation for 90 min, ca. 99% of terbufos was degraded. The photodegradation rate of terbufos was found to increase along with increasing pH and to increase, and then decrease, along with increasing catalyst concentration. In addition, the presence of inorganic ions such as Cl^- and NO_3^- that are often presented in natural water systems decreased the photocatalytic degradation rate of terbufos.

Eight intermediates have been identified and characterized through a mass spectra analysis, giving insight into the early steps of the degradation process. The oxon analogue of terbufos seems to be of the primary product derived from the oxidizing attack of ($^{\bullet}$OH) and the substitution of sulfur by oxygen on the P=S bond. In addition to the degradation route of P=S bond destruction, an alternative pathway was also identified. This pathway could proceed via the formation of terbufos cation radicals by attacking of positive holes initiating the series of reactions. The interfacial transfer of a single electron from the sulfur atom initiates C—S bond cleavage and leads to the formation of the detected intermediates.

The relative photonic efficiency for the photodegradation of terbufos was estimated against phenol as the secondary standard. Actinometer studies resulted in a reaction quantum yield for terbufos of 0.289. The degradation of terbufos was found to follow pseudo-first-order kinetics, and hence the figure-of-merit electrical energy per order (E_{EO}) is appropriate for estimating the electrical energy efficiency. Our study shows that terbufos can be treated easily and effectively with the TiO_2/UV process with E_{EO} value of 71 kWh/(m^3 order).

Acknowledgments

This work was supported by NSC 95-2622-M-438-001-CC3 of the National Science Council of the Republic of China and Tsing-Hua Testing & Analysis Co.

References

[1] K.D. Racke, Degradation of organophosphorus insecticides in environmental matrices, in: J.E. Chambers, P.Z. Levy (Eds.), Organophosphates: Chemistry, Fate, and Effects, Academic Press, San Diego, CA, 1992, pp. 48–78.
[2] M. Jokanovic, Biotransformation of organophosphorus compounds, Toxicology 166 (2001) 139–160.
[3] S.L.M. Juarez, J. Sanchez, Toxicity of the organophosphorus insecticide metamidophos to larvae of the freshwater prawn, Bull. Environ. Contam. Toxicol. 43 (1989) 302–308.
[4] A. Fernandez-Casalderrey, M.D. Ferrando, E. Andreu-Moliner, Endosulfan and diazinon toxicity to the freshwater rotifier Brachionus calyciflorus, J. Environ. Sci. Health B: Pestic. Food Contam. Agric. Wastes 27 (1992) 155–164.
[5] J.-R. Kim, H.-J. Kim, O.-S. Kwon, Acetylcholinesterase and neuropathy target esterase activity in female and male rats exposed to pesticide terbufos, Environ. Toxicol. Pharmacol. 20 (2005) 149–156.
[6] Q. Gan, U. Jans, Nucleophilic reactions of phorate and terbufos with reduced sulfur species under anoxic conditions, J. Agric. Food Chem. 55 (2007) 3546–3554.
[7] U.S. Environmental Protection Agency, 1988. Pesticide fact sheet: Terbufos. Fact Sheet. 5.2. Office of Pesticide Programs, Washington, DC.
[8] C.M. Lee, B. Anderson, A.W. Elzerman, Photochemical oxidation of terbufos, Environ. Toxicol. Chem. 18 (1999) 1349–1353.
[9] F. Hong, K.Y. Win, S.O. Pehkonen, Hydrolysis of terbufos using simulated environmental conditions: rates, mechanisms, and product analysis, J. Agric. Food Chem. 49 (2001) 5866–5873.
[10] G.W. Ware, Fundamentals of Pesticides, Thomson, Fresno, CA, 1986, pp. 34–67.
[11] E. Moctezuma, E. Leyva, G. Palestino, H. de Lasa, Photocatalytic degradation of methyl parathion: reaction pathways and intermediate reaction products, J. Photochem. Photobiol. A: Chem. 186 (2007) 71–84.
[12] H.D. Burrows, M. Canle, J.A. Santaballa, S. Steenken, Reaction pathways and mechanisms of photodegradation of pesticides, J. Photochem. Photobiol. B: Biol. 67 (2002) 71–108.
[13] E. Pelizzetti, V. Maurino, C. Minero, V. Carlin, E. Pramauro, O. Zerbinati, M. Tosato, Photocatalytic degradation of atrazine and other *s*-triazine herbicides, Environ. Sci. Technol. 24 (1990) 1559–1565.
[14] K.H. Wang, Y.H. Hsieh, M.Y. Chou, C.Y. Chang, Photocatalytic degradation of 2-chloro and 2-nitrophenol by titanium dioxide suspensions in aqueous solution, Appl. Catal. B: Environ. 21 (1999) 1–8.
[15] S. Chen, G. Cao, Study on the photocatalytic reduction of dichromate and photocatalytic oxidation of dichlorvos, Chemosphere 60 (2005) 1308–1315.

[16] C.S. Lu, C.C. Chen, F.D. Mai, Y.C. Wu, Photocatalytic degradation of Michler's ethyl ketone in titanium dioxide dispersions under UV irradiation, J. Photochem. Photobiol. A: Chem. 187 (2007) 167–176.
[17] M. Zhou, J. Yu, B. Cheng, Effects of Fe-doping on the photocatalytic activity of mesoporous TiO_2 powders prepared by an ultrasonic method, J. Hazard. Mater. B137 (2006) 1838–1847.
[18] C.-H. Chiou, R.-S. Juang, Photocatalytic degradation of phenol in aqueous solutions by Pr-doped TiO_2 nanoparticles, J. Hazard. Mater. 149 (2007) 1–7.
[19] T. Aarthi, P. Narahari, G. Madras, Photocatalytic degradation of Azure and Sudan dyes using nano TiO_2, J. Hazard. Mater. 149 (2007) 725–734.
[20] C.C. Chen, C.S. Lu, Mechanistic studies of the photocatalytic degradation of methyl green: an investigation of products of the decomposition processes, Environ. Sci. Technol. 41 (2007) 4389–4396.
[21] I.K. Konstantinou, T.A. Albanis, TiO_2-assisted photocatalytic degradation of azo dyes in aqueous solution: kinetic and mechanistic investigations: a review, Appl. Catal. B: Environ. 49 (2004) 1–14.
[22] N. Watanabe, S. Horikoshi, A. Kawasaki, H. Hidaka, N. Serpone, Formation of refractory ring-expanded triazine intermediates during the photocatalyzed mineralization of the endocrine disruptor amitrole and related triazole derivatives at UV-irradiated TiO_2/H_2O interfaces, Environ. Sci. Technol. 39 (2005) 2320–2326.
[23] M.R. Hoffman, S.T. Martin, W. Choi, D.W. Bahnemann, Environmental applications of semiconductor photocatalysis, Chem. Rev. 95 (1995) 69–96.
[24] N. Daneshvar, D. Salari, A.R. Khataee, Photocatalytic degradation of azo dye acid red 14 in water: investigation of the effect of operational parameters, J. Photochem. Photobiol. A: Chem. 157 (2003) 111–116.
[25] D.D. Dionysiou, M.T. Suidan, E. Bekou, I. Baudin, J.M. Laîné, Effect of ionic strength and hydrogen peroxide on the photocatalytic degradation of 4-chlorobenzoic acid in water, Appl. Catal. B: Environ. 26 (2000) 153–171.
[26] C.G. Da Silva, J.L. Faria, Photochemical and photocatalytic degradation of an azo dye in aqueous solution by UV irradiation, J. Photochem. Photobiol. A: Chem. 155 (2003) 133–143.
[27] Y. Zang, R. Farnood, Photocatalytic decomposition of methyl *tert*-butyl ether in aqueous slurry of titanium dioxide, Appl. Catal. B: Environ. 57 (2005) 275–282.
[28] K.E. O'Shea, S. Beightol, I. Garcia, M. Aguilar, D.V. Kalen, W.J. Cooper, Photocatalytic decomposition of organophosphonates in irradiated TiO_2 suspensions, J. Photochem. Photobiol. A: Chem. 107 (1997) 221–226.
[29] S. Malato, J. Blanco, C. Richter, B. Milow, M.I. Maldonado, Solar photocatalytic mineralization of commercial pesticides: methamidophos, Chemosphere 38 (1999) 1145–1156.
[30] M. Kerzhentsev, C. Guillard, J.-M. Herrmann, P. Pichat, Photocatalytic pollutant removal in water at room temperature: case study of the total degradation of the insecticide fenitrothion (phosphorothioic acid *O*,*O*-dimethyl-*O*-(3-methyl-4-nitro-phenyl) ester), Catal. Today 27 (1996) 215–220.
[31] I.K. Konstantinou, T.M. Sakellarides, V.A. Sakkas, T.A. Albanis, Photocatalytic degradation of selected s-triazine herbicides and organophosphorus insecticides over aqueous TiO_2 suspensions, Environ. Sci. Technol. 35 (2001) 398–405.
[32] V.A. Sakkas, D.A. Lambropoulou, T.M. Sakellarides, T.A. Albanis, Application of solid-phase microextraction for monitoring the photocatalytic decomposition of fenthion and parathion in aqueous TiO_2 suspensions, Anal. Chim. Acta 467 (2002) 233–243.
[33] C.C. Chen, C.S. Lu, F.D. Mai, C.S. Weng, Photooxidative *N*-de-ethylation of anionic triarylmethane dye (sulfan blue) in titanium dioxide dispersions under UV irradiation, J. Hazard. Mater. B137 (2006) 1600–1607.
[34] E. Evgenidou, I. Konstantinou, K. Fytianos, T. Albanis, Study of the removal of dichlorvos and dimethoate in a titanium dioxide mediated photocatalytic process through the examination of intermediates and the reaction mechanism, J. Hazard. Mater. B137 (2006) 1056–1064.
[35] S. Rabindranathan, S. Devipriya, S. Yesodharan, Photocatalytic degradation of phosphamidon on semiconductor oxides, J. Hazard. Mater. B102 (2003) 217–229.
[36] X. Zhu, C. Yuan, Y. Bao, J. Yang, Y. Wu, Photocatalytic degradation of pesticide pyridaben on TiO_2 particles, J. Mol. Catal. A 229 (2005) 95–105.
[37] E. Evgenidou, K. Fytianos, I. Poulios, Semiconductor-sensitized photodegradation of dichlorvos in water using TiO_2 and ZnO as catalyst, Appl. Catal. B: Environ. 59 (2005) 81–89.
[38] C.C. Wong, W. Chou, The direct photolysis and photocatalytic degradation of alachlor at different TiO_2 and UV sources, Chemosphere 50 (2003) 981–987.
[39] J. Yu, L. Zhang, B. Cheng, Y. Su, Hydrothermal preparation and photocatalytic activity of hierarchically sponge-like macro-/mesoporous titania, J. Phys. Chem. C 111 (2007) 10582–10589.
[40] J. Yu, X. Zhao, Q. Zhao, Effect of surface structure on photocatalytic activity of TiO_2 thin films prepared by sol–gel method, Thin Solid Films 379 (2000) 7–14.
[41] M. Sökmen, A. Özkan, Decolourising textile wastewater with modified titania: the effects of inorganic anions on the photocatalysis, J. Photochem. Photobiol. A: Chem. 147 (2002) 77–81.
[42] H.Y. Chen, O. Zahraa, M. Bouchy, Inhibition of the adsorption and photocatalytic degradation of an organic contaminant in an aqueous suspension of TiO_2 by inorganic ions, J. Photochem. Photobiol. A: Chem. 108 (1997) 37–44.
[43] J.M. Herrmann, C. Guillard, M. Arguello, A. Agüera, A. Tejedor, L. Piedra, A. Fernández-Alba, Photocatalytic degradation of pesticide pirimiphos-methyl: determination of the reaction pathway and identification of intermediate products by various analytical methods, Catal. Today 54 (1999) 353–367.
[44] K.I. Hadjiivanov, D.G. Klissurski, A.A. Davydov, Study of phosphate-modified TiO_2 (anatase), J. Catal. 116 (1989) 498–505.
[45] C. Zamy, P. Mazellier, B. Legube, Phototransformation of selected organophosphorus pesticides in dilute aqueous solutions, Water Res. 38 (2004) 2305–2314.
[46] J.-T. Li, S.–J. Sheng, X.–L. Du, Metabolism of terbufos in rat liver, J. Occup. Health 41 (1999) 62–68.
[47] R. Nakamura, Y. Nakato, Primary intermediates of oxygen photoevolution reaction on TiO_2 (rutile) particles, revealed by in situ FTIR absorption and photoluminescence measurements, J. Am. Chem. Soc. 126 (2004) 1290–1298.
[48] Y. Murakami, E. Kenji, A.Y. Nosaka, Y. Nosaka, Direct detection of OH radicals diffused to the gas phase from the UV-irradiated photocatalytic TiO_2 surfaces by means of laser-induced fluorescence spectroscopy, J. Phys. Chem. B. 110 (2006) 16808–16811.
[49] E. Kozlova, A. Vorontsov, G. Rima, C. Lion, S. Preis, Photocatalytic oxidation of VX-simulation substance, Water Sci. Technol. 55 (2007) 133–138.
[50] I.K. Konstantinou, T.A. Albanis, Photocatalytic transformation of pesticides in aqueous titanium dioxide suspensions using artificial and solar light: intermediates and degradation pathways, Appl. Catal. B: Environ. 42 (2003) 319–335.
[51] I.K. Konstantinou, V.A. Sakkas, T.A. Albanis, Photocatalytic degradation of the herbicides propanil and molinate over aqueous TiO_2 suspensions: identification of intermediates and the reaction pathway, Appl. Catal. B: Environ. 34 (2001) 227–239.
[52] M.A. Fox, A.A. Abdel-Wahad, Selectivity in the TiO_2-mediated photocatalytic oxidation of thioethers, Tetrahedron Lett. 31 (1990) 4533–4536.
[53] A. Vidal, Z. Dinya, F. Mogyorodi Jr., F. Mogyorodi, Photocatalytic degradation of thiocarbamate herbicide active ingredients in water, Appl. Catal. B: Environ. 21 (1999) 259–267.
[54] A. Dannenberg, S.O. Pehkonen, Investigation of the heterogeneously catalyzed hydrolysis of organophosphorus pesticides, J. Agric. Food Chem. 46 (1998) 325–334.
[55] F. Hong, S.O. Pehkonen, Hydrolysis of phorate using simulated environmental conditions: rates, mechanisms, and product analysis, J. Agric. Food Chem. 46 (1998) 1192–1199.
[56] H.–L. Lien, W.–X. Zhang, Removal of methyl *tert*-butyl ether (MTBE) with Nafion, J. Hazard. Mater. 144 (2007) 194–199.
[57] T. Zhang, T. Oyama, S. Horikoshi, J. Zhao, N. Serpone, H. Hidaka, Photocatalytic decomposition of the sodium dodecylbenzene sulfonate surfactant in aqueous titania suspensions exposed to highly concentrated solar radiation and effects of additives, Appl. Catal. B: Environ. 42 (2003) 13–24.
[58] N. Serpone, G. Sauve, R. Koch, H. Tahiri, P. Pichat, P. Piccinini, E. Pelizzetti, H. Hidaka, Standardization protocol of process efficiencies and activation parameters in heterogeneous photocatalysis: relative photonic efficiencies, J. Photochem. Photobiol. A: Chem. 94 (1996) 191–203.
[59] N. Serpone, Relative photonic efficiencies and quantum yields in heterogeneous photocatalysis, J. Photochem. Photobiol. A: Chem. 104 (1997) 1–12.
[60] N. Daneshvar, A. Aleboyeh, A.R. Khataee, The evaluation of electrical energy per order (E_{Eo}) for photooxidative decolorization of four textile dye solutions by the kinetic model, Chemosphere 59 (2005) 761–767.